Superelectrophiles Stabilized by Phosphorus, Arsenic, and Antimony: Structures and Potential Energy Surface Analysis of PCH_5^{2+}, $AsCH_5^{2+}$, and $SbCH_5^{2+}$

Christoph Widauer, Grace Shiahuy Chen, and Hansjörg Grützmacher*

Dedicated to Professor Hans-Friedrich Grützmacher on the occasion of his 66th birthday

Abstract: We have calculated the homologous series of monocations $[H_2C{=}XH_2]^+$ (**X-1a**, where X = P, As, Sb) and their protonated forms $[H_2C-XH_3]^{2+}$ (**X-2a**) and $[H_3C-XH_2]^{2+}$ (**X-3a**) by use of QCISD levels of theory with pseudopotentials for all X atoms. Refined energies were obtained in CCSD(T) single-point calculations on the QCISD-optimized structures. The structures of the monocations **X-1a** are either planar (X = P) or *trans*-bent (X = As, Sb) with short C–X distances at the QCISD level. Theoretical values for the gas-phase proton affinities (PA) for all monocations show that the formation of either X-site-protonated dications (**X-2a**) or C-site-protonated dications (**X-3a**) is slightly endothermic for X = P and exothermic for X = As, Sb. Since the carbon centers in **X-1a** are negatively charged, as revealed by NBO analyses, X-site- and C-site-protonated isomers of **X-1a** were considered. The X-site-protonated isomer $[H_2C-PH_3]^{2+}$ (**P-2a**) was calculated to be more stable by 3.2 kcal mol^{-1} than the C-site-protonated form **P-3a**. For the As- and Sb-containing dications, the C-site-protonated isomers $[H_3C-AsH_2]^{2+}$ (**As-3a**) and $[H_3C-SbH_2]^{2+}$ (**Sb-3a**) are preferred. Hydrogen-bridged structures (**X-TS**) were found to be transition states for the 1,2-H migration in all cases with activation barriers from X to C of about 8–9 kcal mol^{-1}. The C–X fragmentation of **X-2a** into CH_2^+ and XH_3^+ is exothermic (about -30 kcal mol^{-1}), but hampered by activation barriers in the range 45 (X = P) and 35 kcal mol^{-1} (X = Sb). The dissociation of C-site-protonated **X-3a** into CH_3^+ and the carbene analogues XH_2^+ is even more exothermic. The activation barriers for this reaction are considerably lower (18.8 and 8.2 kcal mol^{-1} for X = P and Sb, respectively). NBO analyses show that charge distributions in all dications are mainly caused by σ charge transfers as a result of electronegativity differences. Within the series of the dications, antimony, the most electropositive element, serves as the most stabilizing α heteroatom, whereas among the monocations, in which π charge donation is very important, the methylenephosphonium ion **P-1a** is more stable than its higher homologues **As-1a** and **Sb-1a**.

Keywords: ab initio calculations · antimony · arsenic · carbocations · phosphorus · superelectrophiles

Introduction

Superelectrophilic activation is responsible for the greatly enhanced reactivity of various α-heteroatom-substituted carbenium ions $[H_{3-n}C(X)_n]^+$ (X = heteroatom or substituent with a heteroatom in the α position).[1a–c] More than thirty years ago, Olah et al. observed that the acetyl cation $MeCO^+$ and the nitronium ion NO_2^+ are much more reactive in superacid media and proposed the formation of the dications $MeCOH^{2+}$ and NO_2H^{2+}, respectively.[2] Vol'pin et al. found that systems like $CBr_4 \cdot 2AlBr_3$, $CHBr_3 \cdot 2AlBr_3$, $CCl_4 \cdot 2AlBr_3$, and $CHCl_3 \cdot 2AlBr_3$ produce superelectrophiles at $-20\,^\circ C$ that catalyze cracking, isomerization, and oligomerization of alkanes and cycloalkanes efficiently.[3] Carboxonium ions $R_2C(OH)^+$ are also strongly activated in superacid media. While highly stabilized $R_2C(OH)^+$ ions do not abstract hydride from alkanes to form carbenium ions (CR_3^+), reaction of $R_2C(OH)^+$ (R = H, Me) with isobutane in presence of HF/SbF_5 or HF/BF_3 leads to the *tert*-butyl cation CMe_3^+.[1a,b] Recently, Olah et al. performed a theoretical and experimental study of the trihalomethyl cations CZ_3^+ (Z = F, Cl, Br, I) and their protonated derivatives.[4a,b] They found that the dications $CBr_2(BrH)^{2+}$ and $CI_2(IH)^{2+}$ are more stable by 15.5 and 44.7 kcal mol^{-1}, respectively, than the monocations CBr_3^+ and CI_3^+. The calculations show that all monoprotonated trihalocarbenium dications are kinetically protected against decomposition into CZ_3^+ and H^+. Moreover, the stability of the protonated halomethyl cations increases in the order Z = F < Cl < Br < I. High-level ab initio studies on the protonation of trichalcogeno-substituted carbenium ions $C(EH)_3^+$ (E = S–Te)[5a–e] show that the formation of the dications $C(EH)_3H^{2+}$ is even more exothermic. Again, the larger

[*] Prof. Dr. H. Grützmacher, C. Widauer, G. S. Chen
Inorganic Chemistry Institute, Swiss Federal Institute of Technology
Universitätsstrasse 6, CH-8092 Zürich (Switzerland)
Fax: (+41) 1-632-10-90
E-mail: gruetz@inorg.chem.ethz.ch

0947-6539/98/0407-1154 $ 17.50+.50/0

exothermicities are found for the heavier chalcogens, selenium and tellurium, and the most stable dication derived by protonation is $C(TeH)_3H^{2+}$. Previously, Radom et al. studied the ylidic dications $[CH_2YH]^{2+}$ and $[CH_3Y]^{2+}$ extensively at the MP3/6-31G**//HF/6-31G* level in which Y = NH_2, OH, F, PH_2, SH and Cl.[6] They considered various dissociation reactions and found that the fragmentation of the tautomers $[H_2C-PH_3]^{2+}$ and $[H_3C-PH_2]^{2+}$ into $[H_2C{=}PH_2]^+$ and H^+ is almost thermoneutral.

In traditional views, the thermodynamic stability of α-heteroatom-substituted carbenium ions, in which the heteroatoms are π donors, is attributed to effective charge dispersal by (p–p)π overlap from the nonbonded electron pair of the heteroelement adjacent to the carbenic center. It was often assumed that elements from the higher periods are poorer π donors as a result of decreasing overlap in the order $2p(\pi)-2p(\pi) > 2p(\pi)-3p(\pi) > 2p(\pi)-4p(\pi) > 2p(\pi)-5p(\pi)$. However, this argument is not supported by calculations,[7a–e] and the increasing number of experimental investigations of carbocations stabilized by α heteroatoms from higher periods (principal quantum number >2) underlines, in agreement with extended ab initio studies, that the heavier elements are at least equally efficient, if not even better, π donors for formally electron-deficient species.[8]

In order to gain a more detailed insight into the electron properties of carbocations and superelectrophiles, we investigated experimentally carbenium ions that are stabilized by a π-donor element from higher periods. We have already reported the preparation and isolation of methylenephosphonium ions $[R_2P{=}CR'_2]^+[A]^-$ (R = *t*Bu; R′ = $SiMe_3$, aryl; A = $AlCl_4$, $SnCl_3$) by abstraction of chlorine from P-halogenated ylides, $R_2ClP{=}CR'_2$.[9a–f] Recently, we succeeded in the preparation and isolation of a set of homologous carbenium ions $C(ER)_3^+$ (E = S, Se, Te; R = 2,4,6-*i*$Pr_3C_6H_2$) where the π-donating α heteroatom could be varied throughout a group in the periodic table.[5a,b] This work was supported by quantum mechanical calculations[5a–c] that confirmed that the heavier elements are not poorer π donors, in accordance with the work of Bernardi et al.[7a] and Schleyer et al.[7e] In continuation of these investigations we now report results of systematic high-level ab initio studies of the pnictogenocarbenium ions $[H_2C{=}XH_2]^+$ (X = P, As, Sb) and their superelectrophilic activation. For the protonated dications $[CH_5X]^{2+}$, we calculated the structures and energies of the two possible isomers $[H_2C-XH_3]^{2+}$ and $[H_3C-XH_2]^{2+}$ with respect to X- and C-site protonations, as well as the transition states of the isomerization. Additionally, we studied the thermodynamic and kinetic stability of the dications. Comparison of the energies of the mono- and dications leads to the proton affinities (PA) for the monocations $[H_2P{=}CH_2]^+$, $[H_2As{=}CH_2]^+$, and $[H_2Sb{=}CH_2]^+$.

Computational Methods

All ab initio calculations were performed with the program package GAUSSIAN 94.[10] The structures of the monocations $[H_2C{=}XH_2]^+$ (X = P, As, Sb) and the dications of $[CH_5P]^{2+}$ were optimized at the full MP2[11] and QCISD[12] levels of theory whereas the geometries of the dications of $[CH_5As]^{2+}$ and $[CH_5Sb]^{2+}$ have been fully optimized at the QCISD(full) level only. The spin-unrestricted UQCISD formalism was used for the open-shell species CH_2^+ and XH_3^+ (X = P, As, Sb). The vibrational frequencies were carried out to characterize the structures as minima or transition states. Relative energies are corrected for vibrational zero-point energies (*V ZPE*, not scaled). Refined energies are obtained at the CCSD(T) level.[13] For C and H the 6-31G* basis set was used.[14] For the heavier atoms P, As, and Sb effective core potentials (ECP) were used with a double-ζ-type valence-electron basis set as described by Bergner et al.[15] and augmented by one set of six Cartesian *d*-type polarization functions with the exponents recommended by Huzinaga et al.[16] The exponents of the *d* functions are 0.340 (P), 0.293 (As), and 0.211 (Sb). The combined basis set is referred to as 6-31G*SECP. For the phosphorus-containing compounds various all-electron basis sets were employed. The results are very similar to those at the QCISD(full)/6-31G*SECP level. Thus, we only focus our discussion on the results obtained by use of the 6-31G*SECP basis set. Atomic charges as well as bond orders and orbital occupancies were obtained at the QCISD(full) level according to Reed and Weinhold's NBO analysis,[17] which is implemented in GAUSSIAN 94.[10] Selected total and relative energies of the monocations $[CH_4X]^+$ and the dications $[CH_5X]^{2+}$ with X = P, As, and Sb are presented in Table 1.

Proton affinities: The gas-phase proton affinity (PA) of a molecule B is defined as the negative reaction enthalpy (PA ≡ $-\Delta H^\circ_{298}$) of the protonation reaction [Eq. (1)] and can be calculated according to Equation (2).[18]

$$B + H^+ \rightarrow BH^+ \quad (1)$$

$$\Delta H_{298} = \Delta E^{elec}_{298} + \Delta E^{vib}_{298} + \Delta E^{rot}_{298} + \Delta E^{trans}_{298} + \Delta(pV)_{298} \quad (2)$$

The electronic energy change for the proton transfer reaction in Equation (1) (ΔE^{elec}_{298}) was computed by means of ab initio methods as described above. The vibrational energy differences (ΔE^{vib}_{298}) were derived from standard statistical mechanical formulae and unscaled vibrational frequencies at the QCISD(full)/6-31G*SECP level. The last three terms in Equation (2) are calculated classically to be $-5RT/2$ for the reaction shown in Equation (1). All calculations were performed for an ideal gas at a constant pressure of 1 atm and a temperature of 298.15 K. Thus, the PA may be written as shown in Equation (3).

$$PA = -\Delta E^{elec}_{298} - \Delta E^{vib}_{298} + 5RT/2 \quad (3)$$

In Scheme 1 the relationship between different products as a result of X- or C-site protonation is shown. The minimum structures of the monocations $[H_2C{=}XH_2]^+$ are denoted as **X-1a** for X = P, As, and Sb. For the minima of the dications, the X-site-protonated species $[H_2C-XH_3]^{2+}$ are labeled as **X-2a** whereas the C-site-protonated species $[H_3C-XH_2]^{2+}$ are labeled as **X-3a** for X = P, As, and Sb.

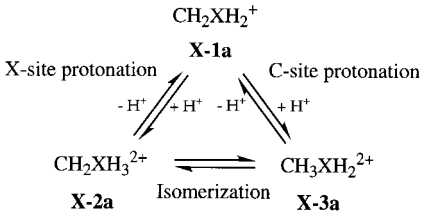

Scheme 1. Schematic presentation of the formation of the two possible isomers **X-2a** and **X-3a** derived from X- and C-site protonation of the monocation **X-1a**.

Results and Discussion

Geometry of the monocations $[CH_2XH_2]^+$: In a recent study, Schleyer et al. investigated $[H_2C{=}XH_2]^+$ for X = N, P, As, and Sb at the MP2 level.[7e] At this level of theory, all monocations $[H_2C{=}XH_2]^+$ prefer planar structures. At the QCISD level, the global minimum of the methylenephosphonium monocation, $[H_2C{=}PH_2]^+$, does indeed correspond to the planar

Table 1. Total vibrational zero-point and relative energies as well as proton affinities PA_{298} for $[CH_4X]^+$ and $[CH_5X]^{2+}$ (X = P, As, Sb).[a]

		MP2(full)/6-31G*SECP				CCSD(T)//QCISD(full)/6-31G*SECP					
	Sym	*E*	*VZPE*	*N*	E_{rel}	*E*	*VZPE*	VE_{298}	*N*	E_{rel}	PA_{298}
P-1a	C_{2v}	– 46.473664	27.1	0	0.0	– 46.512321	26.6	27.2	0	0.0	–
P-1c	C_s	– 46.403510	25.1	1	44.0	– 46.448680	25.0	–	1	38.4	–
P-1d	C_{2v}	– 46.308173	25.0	1	103.9	– 46.344663	25.2	–	1	103.8	–
P-2a	C_s	– 46.475582	32.0	0	0.0	– 46.517759	31.4	32.3	0	0.0	– 0.2
P-2b	C_s	– 46.475443	31.9	1	0.1	– 46.517622	31.3	31.7	1	0.0	0.3
P-3a	C_s	– 46.475452	31.9	0	0.1	– 46.512789	31.6	32.5	0	3.2	– 3.5
P-3b	C_s	– 46.474818	31.9	1	0.5	– 46.512301	31.5	32.0	1	3.6	– 3.3
P-TS	C_s	– 46.462562	31.1	1	8.2	– 46.503835	30.8	31.1	1	8.1	– 7.7
P-SP1	C_s	–	–	–	–	– 46.440024	27.3	–	2[b]	44.7	–
P-SP2	C_s	–	–	–	–	– 46.482327	31.2	–	2[c]	22.0	–
As-1a	C_s	–	–	–	–	– 46.146465	25.5	26.1	0	0.0	–
As-1b	C_{2v}	– 46.109195	25.8	0	0.0	– 46.145999	25.2	–	1	0.0	–
As-1c	C_s	– 46.056364	25.5	1	33.2	– 46.100070	23.9	–	1	27.5	–
As-1d	C_{2v}	– 45.951957	23.8	1	96.6	– 45.987178	24.1	–	1	98.6	–
As-2a	C_s	–	–	–	–	– 46.162592	30.0	31.0	0	0.0	6.8
As-2b	C_s	–	–	–	–	– 46.162516	30.0	30.5	1	0.0	7.2
As-3a	C_s	–	–	–	–	– 46.176009	31.2	32.2	0	7.3	14.0
As-3b	C_s	–	–	–	–	– 46.175924	31.1	31.6	1	7.3	14.5
As-TS	C_s	–	–	–	–	– 46.148161	29.4	29.9	1	8.5	– 1.2
As-SP1	C_s	–	–	–	–	– 46.091462	26.2	–	2[b]	40.8	–
As-SP2	C_s	–	–	–	–	– 46.157330	30.4	–	2[c]	3.7	–
Sb-1a	C_s	–	–	–	–	– 45.339927	23.7	24.4	0	0.0	–
Sb-1b	C_{2v}	– 45.300255	23.9	0	0.0	– 45.337243	23.5	–	1	1.5	–
Sb-1c	C_s	– 45.260970	23.0	1	24.7	– 45.304687	22.2	–	1	20.6	–
Sb-1d	C_{2v}	– 45.167075	21.3	1	83.6	– 45.202307	22.7	–	1	85.4	–
Sb-2a	C_s	–	–	–	–	– 45.373749	27.7	28.9	0	0.0	18.2
Sb-2b	C_s	–	–	–	–	– 45.373721	27.6	28.3	1	0.0	18.8
Sb-3a	C_s	–	–	–	–	– 45.419304	30.3	31.6	0	26.0	44.1
Sb-3b	C_s	–	–	–	–	– 45.419299	30.3	31.0	1	26.0	44.7
Sb-TS	C_s	–	–	–	–	– 45.358817	27.2	27.9	1	9.0	9.8
Sb-SP1	C_s	–	–	–	–	– 45.312068	24.2	–	2[b]	35.2	–
Sb-SP2	C_s	–	–	–	–	– 45.404229	29.0	–	2[c]	17.8	–

[a] Total energies in Hartrees. Vibrational zero-point energy (*VZPE*, not scaled), vibrational energy at 298 K (VE_{298}) and relative energies as well as proton affinities (PA_{298}) in kcal mol^{-1}; *N*: number of imaginary frequencies. [b] The second imaginary frequencies are very small (1.9*i* cm^{-1} for X = P, 2.3*i* cm^{-1} for X = As, and 2.5*i* cm^{-1} for X = Sb). [c] The second imaginary frequencies are very small (4.5*i* cm^{-1} for X = P, 6.6*i* cm^{-1} for X = As, and 6.0*i* cm^{-1} for X = Sb).

structure **P-1a**. In contrast, the global minima for $[H_2C{=}AsH_2]^+$ and $[H_2C{=}SbH_2]^+$ correspond to the C_s-symmetric structures **As-1a** and **Sb-1a** with *trans*-bent conformations ($\Sigma^\circ(As) = 349.6$; $\Sigma^\circ(Sb) = 330.5$). This result is not unexpected in view of the Carter–Goddard–Malrieu–Trinquier (CGMT) model that correlates the singlet–triplet excitation energies ($\Delta E_{S\rightarrow T}$) of the fragments E and E^1, which contain an E=E^1 double bond, with the $\sigma+\pi$ bond strength ($E_{\sigma+\pi}$) of this system.[19a–c] If the inequality $\Sigma\Delta E_{S\rightarrow T} > 1/2\, E_{\sigma+\pi}$ is fulfilled a *trans*-bent structure is expected, whereas a classical-planar structure is predicted if $\Sigma\Delta E_{S\rightarrow T} < 1/2\, E_{\sigma+\pi}$. According to this model, methylenephosphonium ions should have a planar structure, while the increasing stability of the singlet state of the AsH_2^+ and SbH_2^+ fragments and simultaneously decreasing $E_{\sigma+\pi}$ bond energies will bring the nonclassical structure to the fore. They are, however, only slightly stabilized, by 0.02 and 1.5 kcal mol^{-1}, respectively, compared with the planar structures **As-1b** and **Sb-1b**, which are transition states at the QCISD level. All optimized monocation structures are shown in Figure 1.

The transition states **X-1c** and **X-1d**, with X = P, As, and Sb, in which the XH_2 groups are rotated by 90°, have constrained

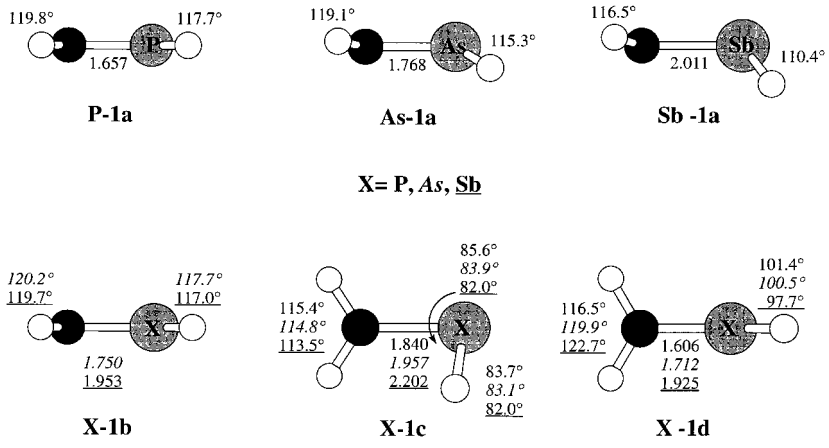

Figure 1. Schematic representation of the structures of the monocations $[H_2C{=}XH_2]^+$ (X = P, As, Sb) together with selected bond lengths [Å] and angles [°]. The minimum structures **X-1a** are depicted separately in order to show the deviation from planarity in **As-1a** and **Sb-1a**. The parameters for the transition states **X-1b**–**X-1d** are given in normal letters for X = P, in italic letters for X = As, and in underlined letters for X = Sb.

0947-6539/98/0407-1156 $ 17.50+.50/0 *Chem. Eur. J.* **1998**, *4*, No. 7

C_s or C_{2v} symmetry. In the C_s-symmetric structures **X-1c** the XH_2 moieties are strongly pyramidalized ($\sphericalangle$CPH = 85.6°; $\Sigma°$(P) = 254.9; $\sphericalangle$CAsH = 83. 9°; $\Sigma°$(As) = 250.8; $\sphericalangle$CSbH = 82.0°; $\Sigma°$(Sb) = 248.6) and bent in such a way that the hydrogen atoms adopt semi-bridging positions between the X and C atoms. They are more stable by 65.5 kcal mol^{-1} for X = P, 71.1 kcal mol^{-1} for X = As, and 64.8 kcal mol^{-1} for X = Sb compared with the corresponding C_{2v}-symmetric species **P-1d**, **As-1d**, and **Sb-1d**, respectively. The phenomenon of partial transfer of the XH_2 hydrogens to the carbon center in the 90°-rotated forms has been previously discussed for $[H_2C{=}PH_2]^+$.[20]

As we expected, the decrease of electronegativity for the heavier pnictogens results in an increase of positive charge on the X-center for the series, P (0.845) < As (0.917) < Sb (1.176). X→C charge transfer by π and σ donation results in a negative partial charge at the carbon atom of −0.664, −0.640, and −0.615 in the singlet ground states of $[H_2C{=}XH_2]^+$ (X = P, As, and Sb, respectively) similiar to halocarbenium ions $[H_2C{-}X]^+$ (X = Cl, Br, and I) in which the carbon center is also negatively charged, but to a lesser extent than in **X-1a**.[5e] The negative charge on the carbon atom diminishes slightly in the order P < As < Sb. If the charges on H_C and H_X are taken into account, and the XH_2 and CH_2 group charges listed in Table 2 are considered, little variation is observed. The group charges are almost equal for all three molecules **X-1a**. The effect of σ charge transfer from the X or C centers to the hydrogens is seen in the change of the σ population for H_C and H_X, which increases for X = P < As < Sb (see Table 3).

Table 3. CH_n and XH_n group charges (n = 2, 3) of the monocations $[H_2C{=}XH_2]^+$ (**X-1a**) and the dications $[H_2C{-}XH_3]^{2+}$ (**X-2a**) and $[H_3C{-}XH_2]^{2+}$ (**X-3a**).

	X–1a		**X–2a**		**X–3a**	
X	CH_2	XH_2	CH_2	XH_3	CH_3	XH_2
P	−0.056	1.057	0.719	1.281	0.139	1.861
As	−0.054	1.057	0.669	1.331	0.080	1.020
Sb	−0.071	1.071	0.556	1.444	0.024	1.976

Protonation of the monocations $[CH_2XH_2]^+$: The optimized dication structures are shown in Figure 2. As noted above, the carbon atoms in $[H_2C{=}XH_2]^+$ have considerable negative charges for all pnictogens. Therefore, we calculated X-site-($[H_2C{-}XH_3]^{2+}$) as well as C-site-protonated structures ($[H_3C{-}XH_2]^{2+}$), **X-2a** and **X-3a**, respectively.

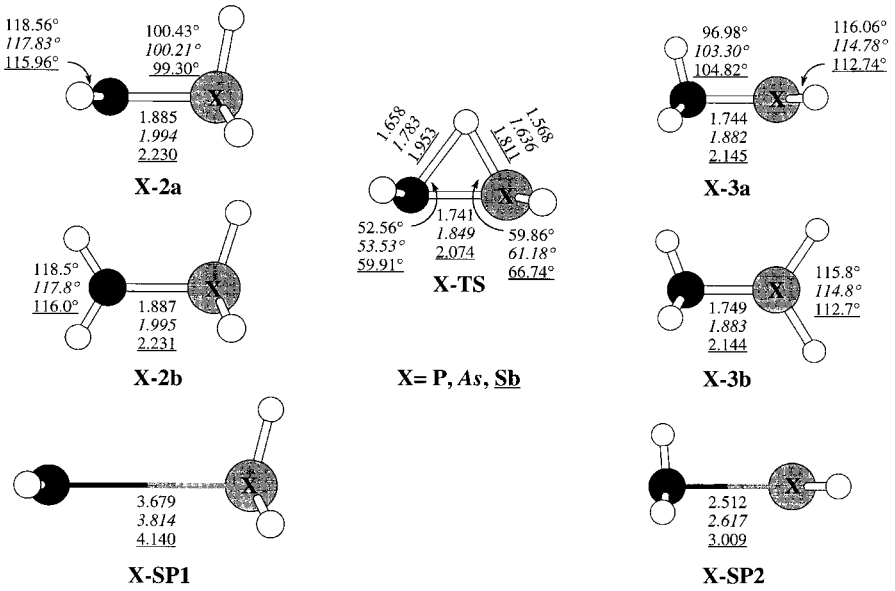

Figure 2. Schematic representation of the structures of the dications $[CH_5X]^{2+}$ (X = P, As, Sb) together with selected bond lengths [Å] and angles [°]. The parameters for all dications **X-2a**–**X-3b** are given in normal letters for X = P, in italic letters for X = As, and in underlined letters for X = Sb.

Table 2. Atomic charges as well as σ and π populations derived from the natural population analysis of the stable conformers of the monocations $[H_2C{=}XH_2]^+$ (**X-1a**) and the dications $[H_2C{-}XH_3]^{2+}$ (**X-2a**) and $[H_3C{-}XH_2]^{2+}$ (**X-3a**).[a]

		X = P			X = As			X = Sb		
	[b]	Charge	σ	π	Charge	σ	π	Charge	σ	π
X-1a	C	−0.667	3.772	0.897	−0.640	3.765	0.876	−0.615	3.822	0.794
	X	0.845	3.026	1.129	0.917	2.984	1.099	1.175	2.789	1.035
	H_C	0.306	0.694	–	0.293	0.707	–	0.272	0.728	–
	H_X	0.106	0.894	–	0.068	0.932	–	−0.052	1.052	–
X-2a	C	0.090	3.830	0.081	0.061	3.867	0.073	−0.020	3.961	0.060
	X	0.718	3.160	1.122	0.882	3.068	1.023	1.350	2.750	0.900
	H_C	0.314	0.686	–	0.304	0.696	–	0.288	0.712	–
	H^1_X	0.195	0.805	–	0.155	0.845	–	0.036	0.964	–
	H^2_X	0.184	0.816	–	0.147	0.853	–	0.029	0.971	–
X-3a	C	−1.108	3.855	1.254	−1.088	3.762	1.327	−1.031	3.686	1.347
	X	1.521	3.191	0.288	1.684	3.147	0.169	2.003	2.913	0.084
	H^1_C	0.439	0.561	–	0.406	0.594	–	0.358	0.642	–
	H^2_C	0.404	0.830	–	0.381	0.882	–	0.349	1.014	–
	H_X	0.170	0.596	–	0.118	0.619	–	−0.018	0.651	–

[a] The NBO analysis were calculated at the QCISD(FULL)/ 6-31G*SECP level. [b] H^1_C denotes the hydrogen connected to C perpendicular to the XH_2 plane. Similarly, H^1_X denotes the hydrogen connected to X perpendicular to the CH_2 plane.

If positive hyperconjugation contributes to the stability of **X-2a** or **X-3a**, pyramidalization of the trigonal coordinated C or X center and narrowing of the HXC or HCX angle that is perpendicular to the CH_2 or XH_2 plane is expected. However, the carbon centers in the dicationic structures **X-2a** are trigonal planar with an angle $\sphericalangle$XCH of 120.7° for X = P, 121.0° for X = As, and 122.0° for X = Sb, and there is no significant bond-angle variation within each species. The π population of the carbon atom in **X-2a** is almost zero for all X atoms indicating that there is no significant π charge transfer in **X-2a** (see Table 3). In this respect, it is interesting to note that in neutral ylides H_2C-XH_3 (X = P, As, Sb), which possess two electrons more, negative hyperconjugation leads to pyramidalization of the carbon center.[21] In the corresponding C-site-protonated minimum structures **X-3a**, the X-center for X = P is slightly pyramidalized indicated by a dihedral angle $H^{\perp}_{C}$CPH of 85.8° for **P-3a**, whereas the X centers in **As-3a** and **Sb-3a** are planar ($H^{\perp}_{C}$CAsH = 88.2°; $H^{\perp}_{C}$CSbH = 89.2°) within the chemical accuracy of the theoretical model ($H^{\perp}_{C}$ denotes the H-atom perpendicular to the XH_2 plane). Additionally, the H–C bond perpendicular to the XH_2 plane forms an $H^{\perp}_{C}$CP bond angle of 97.0° for **P-3a** compared with 103.5° and 104.8° for **As-3a** and **Sb-3a**, respectively. Hence, only in **P-3a** is a notable hyperconjugative interaction observed. The loss of hyperconjugation in the higher homologues is also reflected in the decreasing population of the p(π) orbital on the X center from 0.288 in **P-3a** to 0.169 and 0.084 in **As-3a** and **Sb-3a**, respectively (see Table 3). The twisted structures **X-2b** and **X-3b**, in which the CH_2-groups are rotated by 90°, are all transition states and very close in energy to the corresponding minima. These small energy differences indicate almost free rotation around the C–X bond within the dications $[CH_5X]^{2+}$ (X = P, As, Sb) for both isomers **X-2a** and **X-3a**.

As we can see from Table 1, the PA values increase in the order P < As < Sb regardless of C- or X-site protonation. At the MP2(full)/6-31G*SECP level **P-3a** is only 0.1 kcal mol^{-1} higher in energy than **P-2a**. Inclusion of electron correlation increases this energy difference. As a result, PA values for **P-1a** of −0.2 kcal mol^{-1} and of −3.5 kcal mol^{-1} are obtained, favoring the P-site protonation of $[H_2C{=}PH_2]^+$ over C-site protonation by 3.3 kcal mol^{-1}. On the other hand, for the heavier analogues X = As and Sb, the C-site protonation is increasingly favored over X-site protonation by 7.2 and 25.9 kcal mol^{-1}, respectively. This can be simply explained by the differences in the X–H bond energies, which sharply decrease in the order P > As > Sb.

The charge distributions in the dications have also been calculated from the NBO analyses. In comparison with **X-1a** where the carbon centers are negatively charged (≈ −0.6 e), the total charges of the carbon centers become close to zero in X-site-protonated **X-2a** and decrease from 0.09 for X = P, to 0.06 for X = As, and −0.02 for X = Sb. Concomitantly, the positive charge of X increases from 1.52 for P, to 1.68 for As, and 2.00 for Sb as expected from the decreasing electronegativities. The charge distributions in the C-site-protonated dications **X-3a** are unexpected at first glance. The carbon centers become considerably more negatively charged, when compared with the monocations **X-1a**, while the X-centers bear highly positive charges that increase in the order X = P < As < Sb.

However, with the inclusion of the charges residing on the hydrogen centers in **X-1a**, **X-2a**, and **X-3a**, a somewhat different picture is obtained from comparison of the group charges (Table 2). The CH_2 group in **X-1a** remains negatively charged while the CH_3 groups in **X-3a** bear small positive charges. The +2 charge in these cations is mainly located on the X centers. In the X-site-protonated dications **X-2a**, the charge is more uniformly distributed over the skeleton, but the larger portion of the positive charge remains located on the XH_3 groups as expected. In summary, the trigonal-planar CH_2 units in **X-2a** bear the most positive charge of the hydrocarbon units of all cations studied here, and thus may be designated as activated for nucleophilic attack. In general, in each homologous series of cations, the positive charges on the XH_n groups increase in the order Sb > As > P as electron density is accumulated on the corresponding CH_m units (see Table 2).

Following previous studies by Bernardi et al.[7a] and Schleyer et al.[7e] focusing on the stability of the monocations **X-1a**, we examined the stabilization energies (SE) of the H_3X-onium-substituted dications **X-2a** by application of the isodesmic reaction given in Equation (4). The SE values are presented in Table 4.

$$CH_2XH_n^{(n-1)+} + CH_4 \longrightarrow CH_3XH_n^{(n-2)+} + CH_3^+ \quad (4)$$

Table 4. Stabilization energies SE (kcal mol^{-1}), of the monocations $[H_2C{=}XH_2]^+$ (**X-1a**) and the dications $[H_2C-XH_3]^{2+}$ (**X-2a**) according to the isodesmic reaction given in Equation (4).[a]

X	**X-1a**[b]	**X-2a**
P	57.7 (61.4)	−143.7
As	49.9 (50.7)	−136.9
Sb	45.6 (45.2)	−124.3

[a] All calculated energies at the CCSD(T)/6-31G*SECP//QCISD(FULL)/6-31G*SECP level, inclusive of zero-point energy correction (not scaled). [b] The values given in brackets for **X-1a** are taken from ref. [7e].

We re-examined, at the CCSD(T) level, the stabilization energies for the monocations **X-1a**, which are positive and decrease from 57.7 kcal mol^{-1} for PH_2 over 49.9 kcal mol^{-1} for AsH_2 to 45.6 kcal mol^{-1} for SbH_2. This is in good agreement with the methyl stabilization energies calculated by Schleyer et al.[7e] The reduction of the stabilization energies is rationalized in terms of the cost of planarization energies of trigonal-coordinated X centers, which increase in the order P < As < Sb. This argument can be also used to explain why $[H_2C{=}AsH_2]^+$ and $[H_2C{=}SbH_2]^+$ prefer the *trans*-fold structures **As-1a** and **Sb-1a**. However, the inversion barriers are very low in these ions; this indicates effective π charge transfer in these ions. In contrast, the stabilization energies are strongly negative for the dications **X-2a** and show the inverse trend, that is, they become less exothermic in going from the phosphonium- to the stibonium-substituted dications. In other words, the dication $[H_2C-SbH_3]^{2+}$ is thermodynamically more stable than its arsenic and phosphorus

0947-6539/98/0407-1158 $ 17.50+.50/0 *Chem. Eur. J.* **1998**, *4*, No. 7

analogues. This is not surprising, since protonation of the monocation **X-1a** destroys the π system, and charge transfer in the dications to the formally electron-deficient carbon center is solely due to σ donation, which is most effective for the most electropositive substituent.

Scheme 2 represents the examined potential energy surface of the dications $[CH_5X]^{2+}$ relative to the X-site-protonated dications **X-2a** (X = P, A, Sb). For all three pairs of isomers, we found the C_s-symmetric structures **X-TS** (X = P, As, Sb) as transition states for the isomerization of X- and C-site-protonated species. This is in contrast to the ethyl cation in which the hydrogen-bridged C_{2v} structure corresponds to the

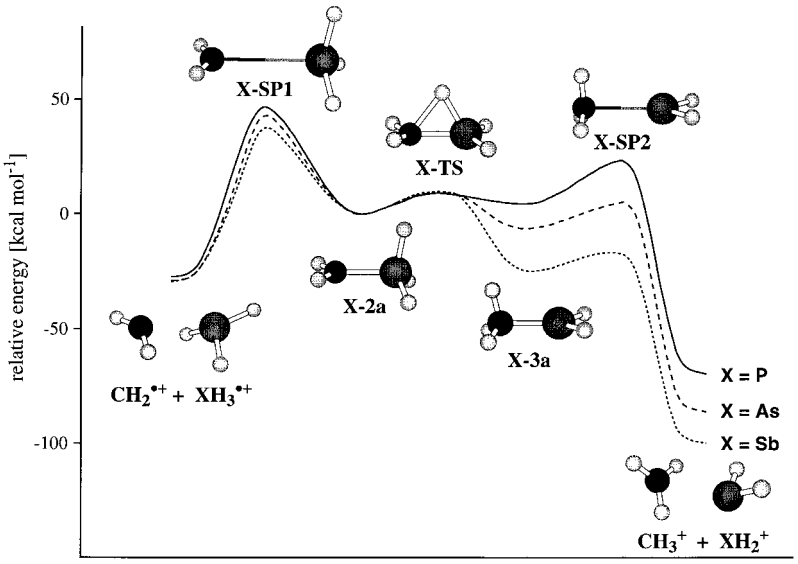

Scheme 2. Schematic energy profile for dissociative processes in the dications $[CH_5X]^{2+}$ with X = P, As, Sb.

global minimum on the energy hypersurface.[22] 1,2-proton migration starting from the X-site-protonated species **X-2a** to the C-site-protonated species **X-3a** is hampered by an energy barrier of about 8–9 kcal mol^{-1} for all X. The energy barrier for the reverse process, that is, 1,2-proton migration from the more stable **X-3a** to **X-2a**, is rather high for X = As (15.8 kcal mol^{-1}) and X = Sb (34.9 kcal mol^{-1}).

Following a suggestion of a referee, we calculated the reaction energies ΔH_{DE} of the C–X bond dissociation according to the reactions given in Equations (5)–(7) in order to study the fragmentation processes for the dications **X-2a** and **X-3a.**

$$[H_2C-XH_3]^{2+} \longrightarrow CH_2^{2+} + XH_3 \quad (5)$$

$$[H_2C-XH_3]^{2+} \longrightarrow CH_2^{\bullet+} + XH_3^{\bullet+} \quad (6)$$

$$[H_3C-XH_3]^{2+} \longrightarrow CH_3^{+} + XH_2^{+} \quad (7)$$

Previous studies by Radom et al. showed that fragmentation of $[CH_5P]^{2+}$ under C–P bond scissions [Eq. (6) and (7)] are exothermic, but are hampered by substantial activation barriers.[6] Our results presented in Table 5 are in general

Table 5. Reaction energies ΔH_{DE} [kcal mol^{-1}] of the C–X fragmentation of the dications **X-2a** the **X-3a** according to the reaction Equations (5)–(7).[a]

X	**X-2a**		**X-3a**
	(5)	(6)	(7)
P	237.8	−28.3 (−27.2)	−73.8 (−65.2)
As	237.2	−30.1	−79.2
Sb	245.7	−30.4	−74.8

[a] All calculated energies at the (U)CCSD(T)/6-31G*SECP//(U)QCISD-(Full)/6-31G*SECP level, inclusive of zero-point energy correction (not scaled). The values in brackets for X = P were obtained at the MP3/6-31G**//(U)HF/6-31G* level (taken from ref. [6]).

agreement with these findings. It is obvious that the heterolytic C–X bond cleavage of **X-2a** into the fragments CH_2^{2+} and XH_3 is highly endothermic for all X (> 230 kcal mol^{-1}). Homolytic C–X bond cleavage of **X-2a** into the radical fragments $CH_2^{\bullet+}$ and $XH_3^{\bullet+}$ is calculated to be exothermic in the range from −28.4 (X = P) to −30.4 kcal mol^{-1} (X = Sb). We were unable to locate the transition states of the C–X fragmentation of **X-2a**. However, second-order saddle points (**X-SP1**) were found that have a second negative frequency of very small magnitude (less than $3i$ cm^{-1}), indicating that the potential-energy surface at the saddle point of the reaction coordinate of the dissociation is very flat. This is caused by the very low energy barrier for the rotation around the C–X bond, which is even less hindered than in the minimum structures **X-2a** owing to the much longer C–X bond distances in **X-SP1**. Therefore, the differences of the total energies of **X-SP1** and **X-2a** can still be taken as a good approximation for the activation barriers of the fragmentation reaction Equation (6). Within these limits, dissociation into the radicals $CH_2^{\bullet+}$ and $XH_3^{\bullet+}$ is strongly hindered by activation barriers of 44.7 kcal mol^{-1} for X = P, 40.8 kcal mol^{-1} for X = As, and 35.2 kcal mol^{-1} for X = Sb.

Decomposition of the C-site-protonated dications **X-3a** into the singlet ground states of the monocationic fragments CH_3^+ and XH_2^+ is exothermic (−73.8 kcal mol^{-1} for X = P, −79.7 kcal mol^{-1} for X = As, and −74.8 kcal mol^{-1} for X = Sb). Again, we could only allocate second-order saddle points **X-SP2** with one negative frequency smaller than $7i$ cm^{-1}. Taking **X-SP2** as approximate transition states, we find considerably smaller activation barriers for the fragmentation in Equation (7) than those for Equation (6), which decrease from 18.8 kcal mol^{-1} for X = P, to 11.0 kcal mol^{-1} for X = As and to 8.2 kcal mol^{-1} for X = Sb.

These results show that although the stability of the dications increase with P < As < Sb, the phosphorus-stabilized dications **P-2a** and **P-3a** are kinetically more persistent against C–X bond dissociation than their heavier homologues. It must be mentioned that all results are discussed for the idealized gas phase and might be different in the condensed phase where electrophilic (protolytic) solvations would be operative.

Conclusions

For the α-heteroatom-substituted carbenium ions $[H_2C{=}XH_2]^+$ (**X-1a**; X = P, As, Sb) protonation is almost thermoneutral for X = P for the formation of dication $[H_3C-PH_2]^{2+}$ (**P-2a**), but increasingly exothermic for X = As, Sb for the formation of dications $[H_3C-AsH_2]^{2+}$ (**As-3a**) and $[H_3C-SbH_2]^{2+}$ (**Sb-3a**) as the more stable isomers. A hydrogen-bridged cyclic structure was found to be a transition state in all cases for the 1,2-hydrogen migration converting X- and C-site-protonated isomers. The charge distribution within the dications can be mainly understood in terms of electronegativity differences and α donation. Thus, it is not surprising that the antimony-substituted C-site-protonated dication, **Sb-3a**, is more stable than its phosphorus analogue, whereas within the series of the monocations **X-1a**, in which π donation is important, an inverse ordering of stabilization (i.e., P > As > Sb) is seen with respect to CH_3^+.[7e] While the stabilization of the monocations suffers from the high planarization energies of the heteroelement center, protonation leading to the dications formally decreases the population of the electron lone pairs at X. Thus X → C π charge transfer becomes unimportant, and the dications are stabilized by α charge transfer, which is largest for the most electropositive element (i.e., antimony). Among all dications studied here the C-site-protonated dication **Sb-3a** is by far the most stable thermodynamically.

Are the dications stable enough against Coulomb explosions, which result from repulsive interactions of the positive charges, to be generated experimentally? Obviously, the heterolytic dissociation of $[H_2C-XH_3]^{2+}$ (**X-2a,** X = P, As, Sb) into H_2C^{2+} and XH_3 will not be a realistic fragmentation pathway since the reaction enthalpies are highly endothermic by more than 230 kcal mol^{-1}. The exothermic (−28 to 30 kcal mol^{-1}) homolytic dissociation into the radicals $CH_2^{\bullet+}$ and $XH_3^{\bullet+}$ is hampered by activation barriers in the range of 35 to 45 kcal mol^{-1}. The dissociation of $[H_3C-XH_2]^{2+}$ (**X-3a,** X = P, As, Sb) into H_3C^+ and the singlet-carbene analogous fragments XH_2^+[19c, 18b] is even more exothermic by about −76 kcal mol^{-1} for all X and less hindered by smaller activation barriers (19 and 8 kcal mol^{-1}). Here, the thermodynamically most stable C-site-protonated dications **As-3a** and **Sb-3a** are kinetically the most labile. It should be possible, however, to generate these dications under suitable conditions (i.e., long-lived stable ions[1a,b]) and use them or their fragmentation products (i.e., XR_2^+ species) as building blocks that possess either a highly electrophilic carbon or a heteroelement center. We are currently performing experiments to verify our theoretical predictions.

Acknowledgements: This work was supported by the Swiss National Science Foundation, the ETH Zürich, and a NATO GRANT (CRG 940399). We thank the referees for their valuable and helpful comments.

Received: August 11, 1997 [F789]

[1] a) G. A. Olah, *Angew. Chem.* **1993**, *105*, 805; *Angew. Chem. Int. Ed. Engl.* **1993**, *32*, 767; b) *ibid.* **1995**, *107*, 1519 and **1995**, *34*, 1393; c) K. Lammertsma, P. von R. Schleyer, H. Schwarz, *ibid.* **1989**, *101*, 1313 and **1989**, *28*, 1321.
[2] G. A. Olah, A. Germain, H. C. Lin, D. A. Forsyth, *J. Am. Chem. Soc.* **1975**, *97*, 2928.
[3] M. Vol'pin, I. Akhrem, A. Orlinkov, *New J. Chem.* **1989**, *13*, 771.
[4] a) G. A. Olah, G. Rasul, L. Heiliger, G. K. S. Prakash, *J. Am. Chem. Soc.* **1996**, *118*, 3580; b) G. A. Olah, G. Rasul, A. K. Yudin, A. Burrichter, G. K. S. Prakash, A. L. Chistayakov, I. V. Stankevich, I. S. Akhrem, N. P. Gambaryan, M. E. Vol'pin, *J. Am. Chem. Soc.* **1996**, *118*, 1446.
[5] a) H. Grützmacher, D. Ohlmann, C. M. Marchand, G. S. Chen, D. Farmer, R. Glaser, A. Currao, R. Nesper, H. Pritzkow, *Angew. Chem.* **1996**, *108*, 317; *Angew. Chem. Int. Ed. Engl.* **1996**, *35*, 300; b) R. Glaser, G. S.-C. Choy, G. S. Chen, H. Grützmacher, *J. Am. Chem. Soc.* **1996**, *118*, 11 617; c) R. Glaser, G. S. Chen, H. Grützmacher, *J. Comp. Chem.* **1997**, *18*, 1023; d) G. S. Chen, R. Glaser, C. M. Marchand, H. Grützmacher, *J. Am. Chem. Soc.* **1997**, in press; e) G. Frenking, S. Fau, C. M. Marchand, H. Grützmacher, *ibid.* **1997**, *119*, 6648.
[6] B. F. Yates, W. J. Bouma, L. Radom, *J. Am. Chem. Soc.* **1986**, *108*, 6545.
[7] a) F. Bernardi, A. Bottoni, A. Venturini, *J. Am. Chem. Soc.* **1986**, *108*, 5395; b) M. W. Schmidt, P. N. Truong, M. S. Gordon, *ibid.* **1987**, *109*, 5217; c) Y. Apeloig, M. Karni, *J. Chem. Soc. Perkin Trans. II* **1988**, 625; d) L. Hevesi, *Phosphorus Sulfur Silicon Relat. Elem.* **1992**, *67*, 155; e) J. Kapp, C. Schade, A. M. El-Nahasa, P. von R. Schleyer, *Angew. Chem.* **1996**, *108*, 2373; *Angew. Chem. Int. Ed. Engl.* **1996**, *35*, 2236.
[8] H. Grützmacher, C. M. Marchand, *Coord. Chem. Rev.* **1997**, *163*, 287.
[9] a) A. Igau, A. Bacereido, H. Grützmacher, H. Pritzkow, G. Bertrand, *J. Am. Chem. Soc.* **1989**, *111*, 6853; b) A. Igau, A. Bacereido, H. Grützmacher, H. Pritzkow, G. Bertrand, *Chem. Eng. News* **1989**, *28*, 24; c) A. Igau, A. Bacereido, H. Grützmacher, H. Pritzkow, G. Bertrand, *Nach. Chem. Tech. Lab.* **1990**, *38*, 185; d) H. Grützmacher, H. Pritzkow, *Angew. Chem.* **1991**, *103*, 721; *Angew. Chem. Int. Ed. Engl.* **1991**, *30*, 709; e) *ibid.* **1992**, *104*, 92 and **1992**, *31*, 99; f) H. Grützmacher, U. Heim, H. Pritzkow, *Phosphorus, Sulfur Relat. Elem.* **1993**, *76*, 21.
[10] M. J. Frisch, G. W. Trucks, H. B. Schlegel, P. M. W. Gill, B. G. Johnson, M. A. Robb, J. R. Cheeseman, T. Keith, G. A. Petersson, J. A. Montgomery, K. Raghavachari, M. A. Al-Alaham, V. G. Zakrzewski, J. V. Ortitz, J. B. Foresman, J. Cioslowski, B. B. Stefanov, A. Nanayakkara, M. Challacombe, C. Y. Peng, P. Y. Ayala, W. Chen, M. W. Wong, J. L. Andres, E. S. Replogle, R. Gomperts, R. L. Martin, D. J. Fox, J. S. Binkley, D. J. Defrees, J. Baker, J. J. P. Stewart, M. Head-Gordon, C. Gonzalez, J. A. Pople, *Gaussian 94, Revision C3*, Gaussian, Pittsburgh, PA, **1995**.
[11] C. Møller, M. S. Plesset, *Phys. Rev.* **1934**, *46*, 618.
[12] J. A. Pople, M. Head-Gordon, K. Raghavachari, *Chem. Phys. Lett.* **1987**, *89*, 7382.
[13] a) G. D. Purvis, R. J. Bartlett, *J. Chem. Phys.* **1982**, *76*, 1910; b) G. E. Scuseria, C. L. Janssen, H. F. Schaefer, III, *ibid.* **1988**, *89*, 7382; c) *idem*, *ibid.* **1989**, *90*, 3700.
[14] M. M. Francl, W. J. Petro, W. J. Hehre, J. S. Binkley, M. S. Gordon, D. J. DeFrees, J. A. Pople, *J. Chem. Phys.* **1982**, *77*, 3654.
[15] A. Bergner, M. Dolg, W. Küchle, H. Stoll, H. Preuss, *Mol. Phys.* **1993**, *80(6)*, 1431.
[16] S. Huzinaga, in *Gaussian Basis Set for Molecular Calculations*, *Vol. 16* (Eds.: J. Andzelm, M. Klobukowski, E. Radzio-Andzelm, Y. Sakai, H. Tatewaki), Elsevier (Amsterdam), **1984**, p. 23.
[17] A. E. Reed, L. A. Curtis, F. Weinhold, *Chem. Rev.* **1988**, *88*, 899.
[18] D. J. DeFrees, A. D. McLean, *J. Comp. Chem.* **1986**, *3*, 321.
[19] a) E. A. Carter, W. A. Goddard, III, *J. Phys. Chem.* **1986**, *90*, 998; b) G. Trinquier, J.-P. Malrieu, *J. Am. Chem. Soc.* **1987**, *109*, 5303; c) M. Driess, H. Grützmacher, *Angew. Chem.* **1996**, *108*, 901; *Angew. Chem. Int. Ed. Engl.* **1996**, *35*, 828.
[20] J. C. White, R. J. Cave, E. R. Davidson, *J. Am. Chem. Soc.* **1988**, *110*, 6308.
[21] D. G. Gilheany, *Chem. Rev.* **1994**, *94*, 1339.
[22] K. Raghavachari, R. A. Whiteside, J. A. Pople, P. von R. Schleyer, *J. Am. Chem. Soc.* **1981**, 103, 5649.

  0947-6539/98/0407-1160 $ 17.50+.50/0